# ICAM-directed vascular immunotargeting of antithrombotic agents to the endothelial luminal surface

Juan-Carlos Murciano, Silvia Muro, Lauren Koniaris, Melpo Christofidou-Solomidou, David W. Harshaw, Steven M. Albelda, D. Neil Granger, Douglas B. Cines, and Vladimir R. Muzykantov

**Drug targeting to a highly expressed, noninternalizable determinant up-regulated on the perturbed endothelium may help to manage inflammation and thrombosis. We tested whether inter-cellular adhesion molecule-1 (ICAM-1) targeting is suitable to deliver antithrombotic drugs to the pulmonary vascular lumen. ICAM-1 antibodies bind to the surface of endothelial cells in culture, in perfused lungs, and in vivo. Proinflammatory cytokines enhance anti-ICAM binding to the endothelium without inducing internalization. $^{125}$I-labeled anti-ICAM and a reporter enzyme (β-Gal) conjugated to anti-ICAM bind to endothelium and accumulate in the lungs after intravenous administration in rats and mice. Anti-ICAM is seen to localize predominantly on the luminal surface of the pulmonary endothelium by electron microscopy. We studied the pharmacological effect of ICAM-directed targeting of tissue-type plasminogen activator (tPA). Anti-ICAM/tPA, but not control IgG/tPA, conjugate accumulates in the rat lungs, where it exerts plasminogen activator activity and dissolves fibrin microemboli. Therefore, ICAM may serve as a target for drug delivery to endothelium, for example, for pulmonary thromboprophylaxis. Enhanced drug delivery to sites of inflammation and the potential anti-inflammatory effect of blocking ICAM-1 may enhance the benefit of this targeting strategy. (Blood. 2003;101:3977-3984)**



## Introduction

Thrombosis and inflammation are often intertwined processes that contribute to cardiovascular morbidity and mortality. In many cases, the pulmonary vasculature is the major site of vascular inflammation and thrombosis, and considerable efforts have been expended to develop strategies to target drugs to this site. Yet current methods to manage inflammation-related thrombosis remain suboptimal.[1-3] For example, targeting fibrin and activated platelets promotes the delivery of antithrombotic agents to existing blood clots, for example, in coronary vessels.[4,5] However, targeting components of preformed clots has afforded only modest improvements in experimental models, likely due to limited penetration,[6] and such clot-targeting strategies are unlikely to be useful for thromboprophylaxis.

Targeted delivery of antithrombotic drugs to the vascular lumen, including those involved by inflammation, prior to clot formation may permit thromboprophylaxis in patients with a high propensity for thrombosis. Theoretically, overexpression of certain antithrombotic proteins by vascular endothelial cells themselves would help to achieve this goal.[7-9] However, gene therapies currently are not suitable to manage acute conditions.[10]

Immunotargeting of therapeutic proteins may provide a complementary strategy suitable for more immediate interventions. Antibodies to diverse determinants are being explored as affinity carriers for drug targeting to endothelium.[11-15] A poorly internalizable, high-density, and stably exposed determinant on the endothelial surface, up-regulated and functionally involved in vascular thrombosis and inflammation, would provide an ideal target for antithrombotic proteins. Previous data indirectly suggest that inter-cellular adhesion molecule-1 (ICAM) may provide such a target to deliver anti-inflammatory and, perhaps, antithrombotic agents.[16-20] However, neither the endothelial internalization of ICAM antibodies (anti-ICAM) nor the tissue distribution, localization, activity, and effects of ICAM-targeted therapeutics have been characterized.

In this work we studied ICAM-directed immunotargeting to endothelium in cell cultures, perfused lungs, and animals, and found that (1) anti-ICAM is not internalized efficiently by the endothelium, (2) cytokine up-regulation of ICAM expression augments surface targeting, but not internalization, of anti-ICAM, (3) anti-ICAM can be used to produce either internalizable (100-200 nm diameter) or noninternalizable (approximately 1 μm) conjugates, and (4) ICAM targeting delivers active tPA to the pulmonary vascular lumen and facilitates intravascular fibrinolysis.

## Materials and methods

The materials used were $Na^{125}I$ and $Na^{131}I$ from Perkin-Elmer (Boston, MA), iodogen, streptavidin (SA), and 6-biotinylaminocaproic acid N-hydroxysuccinimide ester from Pierce (Rockford, IL), human recombinant tPA from Genentech (San Francisco, CA), β-galactosidase-streptavidin

From the Institute of Environmental Medicine, Department of Pharmacology, Department of Medicine, Department of Pathology and Laboratory Medicine, University of Pennsylvania, Philadelphia, PA; and the Department of Physiology, Louisiana State University, Shreveport, LA.

Submitted September 18, 2002; accepted January 7, 2003. Prepublished online as *Blood* First Edition Paper, January 16, 2003; DOI 10.1182/blood-2002-09-2853.

Supported by NIH SCOR in Acute Lung Injury (NHLBI HL 60290, Project 4, NHLBI RO1 HL/GM 71175-01) and a Department of Defense Grant (PR 012262) to V.R.M., grants HL60169 and R03 TW01468 to D.B.C., a fellowship from the Spanish Ministry of Education and Science (MEC) to J.-C.M., and Fundación Ramón Areces (Spain) (S.M.). M.C.-S. was supported in part by the American Heart Association.

Presented in part as posters at the American Thoracic Society (ATS) Meeting, May 5-10, 2000, Toronto, ON, Canada.

**Reprints:** Vladimir Muzykantov, Institute for Environmental Medicine, University of Pennsylvania, School of Medicine, 1 John Morgan Building, Philadelphia, PA 19104-6068; e-mail: muzykant@mail.med.upenn.edu.

The publication costs of this article were defrayed in part by page charge payment. Therefore, and solely to indicate this fact, this article is hereby marked "advertisement" in accordance with 18 U.S.C. section 1734.

conjugate (SA-β-Gal) from Sigma (St Louis, MO), chromogenic tPA substrate, Spectrozyme tPA, a kind gift from American Diagnostica (Greenwich, CT), and fluorescein-labeled transferrin or SA from Molecular Probes (Eugene, OR). Monoclonal (IgG) antibodies were mAb R6.5,[21] mAb 1A29,[22] and mAb YN1[23] against human, rat, and murine ICAM-1; mAb 9B9 against human and rat angiotensin-converting enzyme (ACE)[24]; and mAb 1009 and mAb 311 against human and murine thrombomodulin, TM.[11] Antibodies against IgG (fluorescent-labeled or gold-conjugated) were from Jackson Immunoresearch (West Grove, PA) and Amersham (Piscataway, NJ).

### Conjugation and size determination

Antibodies, IgG, and tissue-type plasminogen activator (tPA) were biotinylated and radiolabeled using Iodogen without loss of activity, as described.[25] The number of biotin residues per molecule of protein was determined by Immunopure-HABA assay (Pierce) as per manufacturer instructions. Biotinylated tPA or β-Gal was coupled to biotinylated antibodies using streptavidin cross-linking following a 3-step procedure described in detail previously.[25-27] The size of the resulting conjugates was determined by dynamic light scattering, as described.[25-27] The conjugates are designated hereafter as anti-ICAM/β-Gal and IgG/β-Gal or anti-ICAM/tPA and IgG/tPA.

### Cell culture experiments

Surface binding and intracellular uptake of $^{125}$I-labeled antibodies were measured in cultures of human umbilical vein endothelial cells (HUVECs, from Clonetics) and a human mesothelioma cell line expressing ICAM-1 (REN cells) as described previously for anti–platelet-endothelial cell adhesion molecule (PECAM).[28] Control and tumor necrosis factor α (TNFα)–challenged cells were incubated for 1 hour at either 4°C or 37°C with $^{125}$I–anti-ICAM, $^{125}$I–anti-ACE, $^{125}$I–anti-TM, or $^{125}$I–control IgG. After washing, surface-bound antibodies were eluted with glycine, while internalized antibodies were measured in the cell lysates.

Suspended control or TNFα-treated HUVEC and REN cells were incubated with 30 μg/mL anti-ICAM or anti-TM for 1 hour at 4°C, washed, counterstained with fluorescein isothiocyanate (FITC)–labeled goat anti–mouse IgG (30 minutes at 4°C), resuspended in phosphate-buffered saline (PBS), and analyzed by fluorescence-activated cell-sorter scanner (FACS).

Cellular localization of anti-ICAM was visualized using immunofluorescence at magnification × 60 or × 40. TNFα-treated cells were incubated with 10 μg/mL anti-ICAM for 1 hour at either 4°C or 37°C in 1% bovine serum albumin (BSA)–containing medium. After washing and fixation, the surface-associated anti-ICAM was stained with Texas Red–labeled goat anti–mouse IgG. Thereafter, internalized anti-ICAM was counterstained in permeabilized cells using FITC-labeled goat anti–mouse IgG. Fluorescein-labeled transferrin was used as a control for internalizable ligand in parallel wells. In separate experiments, rat pulmonary microvascular endothelial cells (RPMVECs) were incubated with anti-ICAM/SA–Texas Red conjugates of different sizes (100-200 nm or approximately 1 μm) for 1 hour at 37°C. After cell fixation, surface-bound conjugates were counterstained with an FITC-labeled goat anti–mouse IgG.

### Experiments in isolated perfused rat lungs (IPL)

Lungs were isolated from anesthetized male 170-200 g Sprague-Dawley rats following protocols approved by the University of Pennsylvania Institutional Animal Care and Use Committee (IACUC) and were ventilated and perfused for 1 hour at 37°C or 4°C with Krebs ringer buffer (KRB)–BSA buffer containing $^{125}$I-labeled antibodies (1 μg, unless indicated otherwise), followed by nonrecirculating perfusion with KRB-BSA, as described.[29,30] In separate experiments, 100 μg nonradiolabeled, biotinylated anti-ICAM or anti-ACE was perfused for 1 hour at 37°C. $^{125}$I-labeled streptavidin ($^{125}$I-SA) was added to the perfusate immediately after washing the unbound antibody or after an additional 60 minutes of nonrecycling perfusion to measure surface-accessible b–anti-ICAM.

### $^{125}$I–anti-ICAM biodistribution in rats

Anesthetized rats and mice were killed 1 hour after a tail-vein injection of a mixture of $^{125}$I–anti-ICAM and $^{131}$I-IgG (10 μg each), and the radioactivity in blood and major organs (washed with saline, blotted dry, and weighed) was measured to calculate the parameters of targeting: percent of injected dose per organ (%ID) or per gram (%ID/g), organ-to-blood ratio (localization ratio, LR), and immunospecificity index (ISI) (see Murciano et al[29] and Danilov et al[31] for details).

### Biodistribution and tissue localization of anti-ICAM and anti-ICAM/β-Gal conjugates in animals

The tissue localization of enzymatically active anti-ICAM/β-Gal 1 hour after the tail-vein injection of 100 μg conjugate in BALB/c mice was visualized by histological analysis of X-Gal staining in the tissues, as described previously for anti-PECAM/β-Gal conjugate.[26] In a similar experiment, lungs were processed for electron microscopy and developed using a gold-conjugated secondary antibody, as described.[26]

### Characterization of tPA activity in lung tissue

Anti-ICAM/tPA conjugate or control preparations (IgG/tPA and tPA) were perfused in IPL for 1 hour; unbound materials were eliminated by a 5-minute nonrecycling perfusion. In one series, lungs were perfused with 3 μg $^{125}$I-labeled tPA conjugated to either anti-ICAM or IgG, and the radioactivity was measured. In the next series, aliquots of lung homogenates obtained after perfusion of 100 μg of unlabeled tPA conjugates were added to $^{125}$I-labeled fibrin clots, formed as described previously,[30] and the release of $^{125}$Iodine into the supernatant at 37°C was measured. In the next series, 750 μL of a 0.4 mM/L solution of a chromogenic tPA substrate was infused into the lung via the pulmonary artery for 20 minutes, and the optical density at 405 nm in the outflow perfusate was measured. In the last series, a suspension of $^{125}$I-labeled fibrin microemboli ($^{125}$I-ME, 3-10 micron diameter), prepared as described previously,[32] was infused into the common pulmonary artery after perfusion with either anti-ICAM/tPA or IgG/tPA. $^{125}$I-ME lodge and degrade slowly in intact isolated perfused rat lungs.[30] The lungs were perfused for 1 hour with buffer containing 20% plasma as a source of plasminogen, and the residual radioactivity in the lungs was measured.

### Statistics

A *t* test or a one-way analysis of variance (ANOVA) (SigmaStat 2.0) was used to determine statistically significant differences ($P < .05$) between groups. Post hoc testing was performed with Fisher Least Square difference test. Data are shown as mean ± SEM unless otherwise stated.

## Results

### Endothelial cells internalize anti-ICAM inefficiently

$^{125}$I–anti-ICAM, but not control IgG, bound specifically to unstimulated endothelial cells (HUVECs) (Figure 1A). Eighty-five percent of the $^{125}$I–anti-ICAM bound to cells at 37°C was eluted by glycine one hour later, compared with 90%-95% bound at 4°C (not shown).

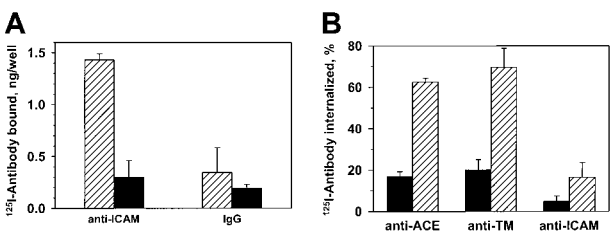


**Figure 1. Resting endothelial cells bind but do not internalize $^{125}$I–anti-ICAM.** (A) HUVECs were incubated with $^{125}$I–anti-ICAM or $^{125}$I-IgG (1 hour, 37°C), and radioactivity was determined in the surface fraction (glycine elution, ▨) and in the cell lysates (■). (B) Percent of internalization of $^{125}$I-labeled antibodies against ACE, TM, and ICAM-1 by HUVECs at either 4°C (■) or 37°C (▨). The data are expressed as means ± SD (n = 3).

Consistent with this, approximately 10% of bound anti-ICAM was internalized by 60 minutes at 37°C versus approximately 60% of $^{125}$I–anti-ACE and $^{125}$I–anti-TM (Figure 1B). Therefore, resting endothelial cells internalize anti-ICAM inefficiently, leaving approximately 90% of the antibody on the cell surface.

### Anti-ICAM uptake in the perfused rat lungs (IPL)

We then asked whether anti-ICAM was handled similarly by intact vascular endothelium under flow. Rat IPLs were perfused with $^{125}$I–anti-ICAM or control $^{125}$I-IgG in a blood-free buffer. $^{125}$I–anti-ICAM bound specifically to the lungs (Figure 2A), reaching saturation at approximately 10 μg per gram of tissue. Scatchard analysis (inset) revealed that rat lungs contain approximately $5 \times 10^{13}$ anti-ICAM binding sites per gram (approximately 1.5-$2.5 \times 10^5$ binding sites per endothelial cell).

We then examined the internalization of anti-ICAM and anti-ACE in IPL. Pulmonary uptake of $^{125}$I–anti-ACE was markedly lower at 6°C than at 37°C, likely due to inhibition of the energy-dependent uptake of antibody. In contrast, practically the same uptake of $^{125}$I–anti-ICAM was seen at 6°C and at 37°C (Figure 2B). This result reflects minor, if any, contribution of an energy-dependent internalization pathway for anti-ICAM in IPL.

The IPL setting permits sequential perfusion of $^{125}$I-SA immediately or 1 hour after biotinylated antibodies, to test the accessibility of endothelium-bound antibodies to the circulation. Binding of $^{125}$I-SA in the lungs was reduced by 70% when biotinylated anti-ACE was allowed to remain in the vasculature for 1 hour at 37°C, indicating antibody disappearance from the lumen. In contrast, binding of $^{125}$I-SA after perfusion of biotinylated anti-ICAM did not diminish with time, indicating that the endothelium-bound anti-ICAM remains accessible from the lumen at 37°C (Figure 2C). Therefore, pulmonary endothelium under flow conditions avidly binds but internalizes anti-ICAM poorly.

### TNFα stimulates anti-ICAM binding, but not internalization

TNFα augmented anti-ICAM binding to HUVECs but inhibited anti-TM binding, while REN cells, which do not express thrombomodulin, bound anti-ICAM constitutively at a relatively high level that was augmented further by TNFα (FACS analysis, Figure 3A).

FACS results were confirmed by $^{125}$Iodine tracing studies using HUVEC monolayers. TNFα markedly augmented binding of $^{125}$I–anti-ICAM but not control $^{125}$I-IgG (Figure 3B). However, the intracellular uptake of $^{125}$I–anti-ICAM by TNFα-stimulated cells after a 1-hour incubation at 37°C was equivalent in HUVEC (11.6% ± 0.7%) and REN cells (10.1% ± 2.7%); background levels at 4°C were 5.1% ± 0.8% and 3.2% ± 0.6%, respectively.

These radiotracer data showing minimal (no more than 10%) internalization of anti-ICAM by cytokine-stimulated cells were confirmed by immunofluorescence microscopy. Figure 3C shows typical images of TNFα-stimulated HUVEC and REN cells

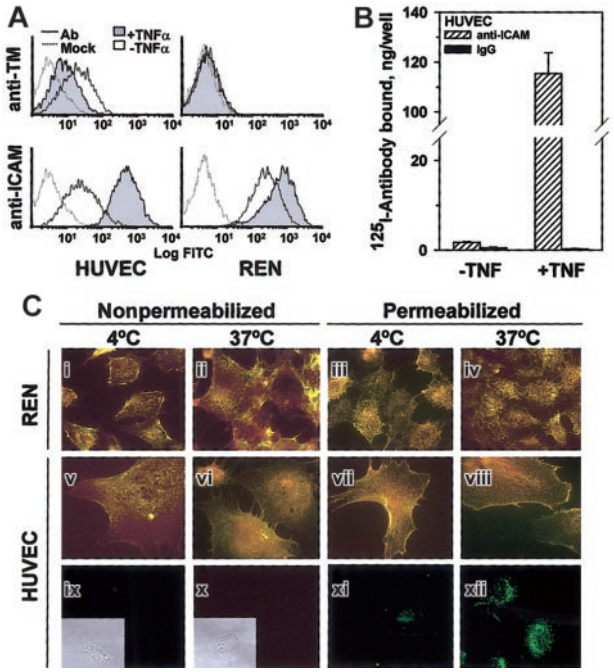


**Figure 3. TNFα increases anti-ICAM binding but not internalization by endothelial and mesothelioma cells.** (A) FACS analysis using anti-ICAM and anti-TM. TNFα suppresses expression of thrombomodulin (TM, upper panels) by HUVECs and stimulates that of ICAM-1 (lower panels) by HUVEC and REN cells. Dashed line: antibody-free medium; resting (open histogram) or TNFα-challenged (shaded histogram) cells. (B) $^{125}$I–anti-ICAM binding to resting and TNFα-treated HUVEC monolayer. The data are shown as means ± SD, n = 4. (C) Fluorescent micrographs (× 60) of TNFα-stimulated cells incubated with anti-ICAM. The cells were incubated at 4°C or 37°C with anti-ICAM (panels i-viii), antibody-free medium (ix, x) or transferrin (xi, xii). After washing and fixation the cells were sequentially stained with Texas Red secondary antibody, permeabilized, and counterstained with FITC-labeled secondary antibody (yellow, surface-bound anti-ICAM; green, internalized anti-ICAM). On the left, the nonpermeabilized cells were stained with both Texas Red and FITC-labeled antibodies (positive control for surface staining, yellow color). Green color corresponds to the intracellular staining (see panels xi and xii showing staining of HUVECs incubated with fluorescein-labeled transferrin). Insets of subpanels ix and x show phase contrast images in controls. Original magnification, × 60; insets minimized to ⅓ of original size.

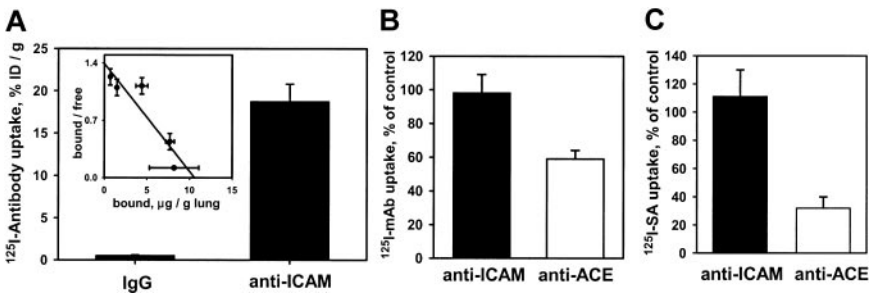


**Figure 2. $^{125}$I–anti-ICAM accumulates without internalization in the isolated rat lungs.** (A) Accumulation of $^{125}$I–anti-ICAM or $^{125}$I-IgG perfused for 1 hour at 37°C. Inset shows a Scatchard analysis of $^{125}$I–anti-ICAM binding. (B) Temperature dependence of anti-ICAM uptake (■) and anti-ACE uptake (□) in the lungs. At 4°C, the pulmonary uptake of $^{125}$I–anti-ACE is inhibited, whereas the uptake of $^{125}$I–anti-ICAM is not affected (uptake at 4°C is shown as percent of the 100% control value attained at 37°C). (C) Disappearance of anti-ICAM (■) and anti-ACE (□) from the luminal surface in the lungs perfused at 37°C. After accumulation in the lungs, biotin–anti-ICAM, but not biotin–anti-ACE, is accessible to the blood for a prolonged time. $^{125}$I-streptavidin ($^{125}$I-SA) was perfused in the lungs either immediately after biotinylated antibody accumulation or after 60 minutes of additional perfusion at 37°C with antibody-free buffer. Data of $^{125}$I-SA uptake after 60 minutes delay are shown as percent of that observed immediately after biotinylated antibody accumulation (100% level). All data are shown as means ± SEM; n = 4.

incubated with anti-ICAM for 1 hour at either 4°C or 37°C and stained before or after permeabilization with Texas Red and FITC-labeled secondary antibody. The staining of intact and permeabilized cells was essentially identical, showing predominantly dual (yellow) labeling of the surface-bound anti-ICAM both at 4°C and 37°C, with no appreciable green staining (representing internalized anti-ICAM). As a control, the intracellular staining of HUVECs incubated with internalizable fluorescein-labeled transferrin was evident at 37°C but not at 4°C (Figure 3Bxi-xii). Therefore, TNFα markedly up-regulates anti-ICAM binding to endothelial and mesothelial cells, but does not augment anti-ICAM internalization.

### Biodistribution of radiolabeled anti-ICAM in vivo

$^{125}$I–anti-ICAM, but not $^{131}$I-IgG, accumulated in the lungs after intravenous injection in rats (Figure 4) and in mice (not shown). Significant uptake also was seen in the liver and spleen, but anti-ICAM uptake per gram of tissue was always greatest in the lungs. Pulmonary uptake of anti-ICAM was 20%-30% lower after intra-arterial injection (not shown).

We analyzed the specificity of anti-ICAM targeting to pulmonary tissue. In rats, the pulmonary uptake of $^{125}$I–anti-ICAM was approximately 17% ID/g (Figure 4A), an immunospecificity index ($ISI_{\%ID/g}$, ratio of %ID/g of anti-ICAM to that of IgG) of approximately 25, 10-fold higher than that in the liver and spleen (Figure 4B). The blood level of anti-ICAM was lower than that of control IgG, likely due to depletion of the circulating pool. The anti-ICAM pulmonary localization ratio (LR, tissue-to-blood ratio) was approximately 50 (Figure 4C), while the IgG LR was approximately 0.2. Therefore, the pulmonary $ISI_{LR}$ calculated using anti-ICAM and IgG LR, thereby correcting for the blood level, was approximately 250 (Figure 4D).

### Effects of proinflammatory challenges on anti-ICAM targeting

Endotoxin facilitated pulmonary uptake of $^{125}$I–anti-ICAM, likely due to up-regulation of endothelial ICAM in response to cytokines. In rats, lipopolysaccharide (LPS) caused a 30% increase in the pulmonary uptake of $^{125}$I–anti-ICAM (Figure 5), with a concomitant reduction in the blood level (pulmonary LR almost doubled from 50 to 85). In contrast, LPS suppressed pulmonary uptake of $^{125}$I–anti-ACE in rats by 50% (pulmonary LR reduced from 14 to 7). Therefore, anti-ICAM targeting in LPS-treated rats was 10 times more robust than that of anti-ACE (LR 85 vs 7). Pulmonary targeting of $^{125}$I–anti-ICAM was stably enhanced at 5 and 24 hours after LPS injection (LR 77 and 85). A similar elevation of

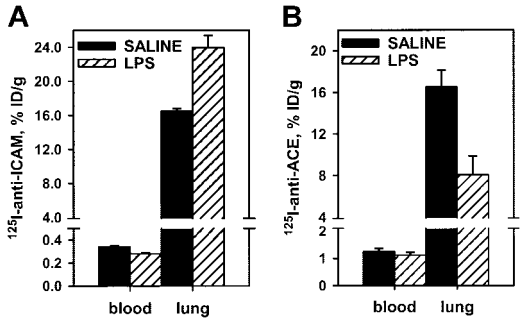


**Figure 5. Endotoxin enhances $^{125}$I–anti-ICAM pulmonary targeting.** $^{125}$I–anti-ICAM (left panel) or $^{125}$I–anti-ACE (right panel) was injected in control rats (black bars) or after intraperitoneal injection of LPS (hatched bars). Lung and blood level of $^{125}$I was determined 1 hour later. Data are presented as means ± SEM, n = 4.

$^{125}$I–anti-ICAM pulmonary targeting was seen in LPS-treated mice (not shown). The $^{125}$I–anti-ICAM pulmonary uptake was doubled in mice exposed to 98% $O_2$ atmosphere, in contrast with a 50% decrease in the $^{125}$I–anti-TM uptake (not shown). Therefore, proinflammatory factors suppress anti-ACE and anti-TM but augment anti-ICAM targeting.

### Visualization of ICAM-directed vascular immunotargeting in animals

We visualized the pulmonary localization of anti-ICAM in mice by electron microscopy. Specific binding of the secondary gold-labeled antibody was evident in lungs harvested 4 hours after anti-ICAM injection (Figure 6A). Semiquantitative analysis after anti-ICAM injection revealed 16 ± 3 endothelium-associated particles/field versus 3 ± 1 particles/field associated with alveolar epithelium and interstitium (M ± SEM, 10 fields). Anti-ICAM was primarily localized along the luminal surface of the endothelium (arrows in Figure 6Ai). Noteworthy, we did not see endocytic vacuoles containing gold particles, the hallmark of endothelial uptake of internalizable conjugates in the lungs.[26]

To test whether anti-ICAM delivers an active enzyme cargo to endothelium, we conjugated a reporter enzyme, β-galactosidase, with anti-ICAM or control IgG. Figure 6B shows the results of X-Gal staining of the organs 1 hour after injection of either anti-ICAM/β-Gal or IgG/β-Gal conjugate in mice. After IgG/β-Gal injection (Figure 6Bv-viii), β-Gal activity was seen in the peripheral zone of the splenic follicles, the known site of Fc-receptor mediated uptake of immunoconjugates.[26,33] The splenic follicles also were stained by anti-ICAM/β-Gal (Figure 6Bi), as

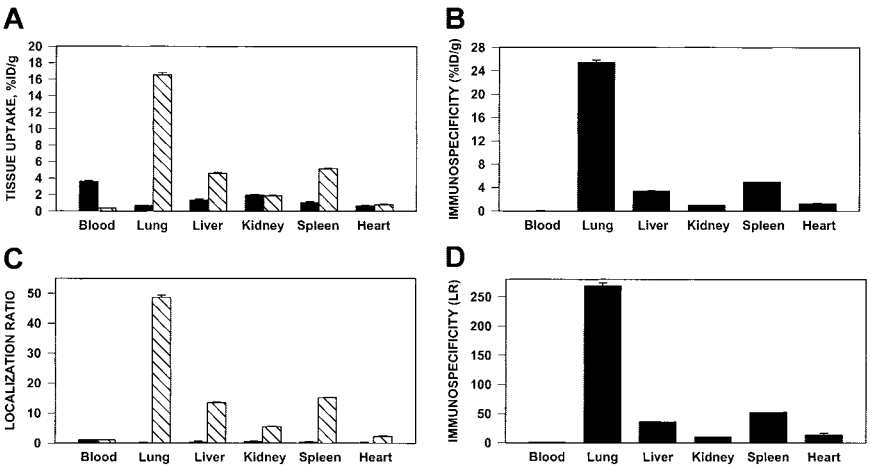


**Figure 4. Pulmonary targeting of $^{125}$I–anti-ICAM in rats.** Biodistribution of $^{125}$I–anti-ICAM (▨) or $^{131}$I-IgG (■) 1 hour after intravenous injection in anesthetized rats. The data are shown as means ± SEM, n = 4. (A) Absolute values of the uptake in organs expressed as percent of injected dose per gram. (B) Immunospecificity index ($ISI_{\%ID/g}$), calculated as ratio of anti-ICAM to IgG %ID/g. (C) Localization ratio (LR) calculated as ratio of %ID/g in an organ to that in blood. (D) $ISI_{LR}$ calculated as ratio of anti-ICAM LR to IgG LR.

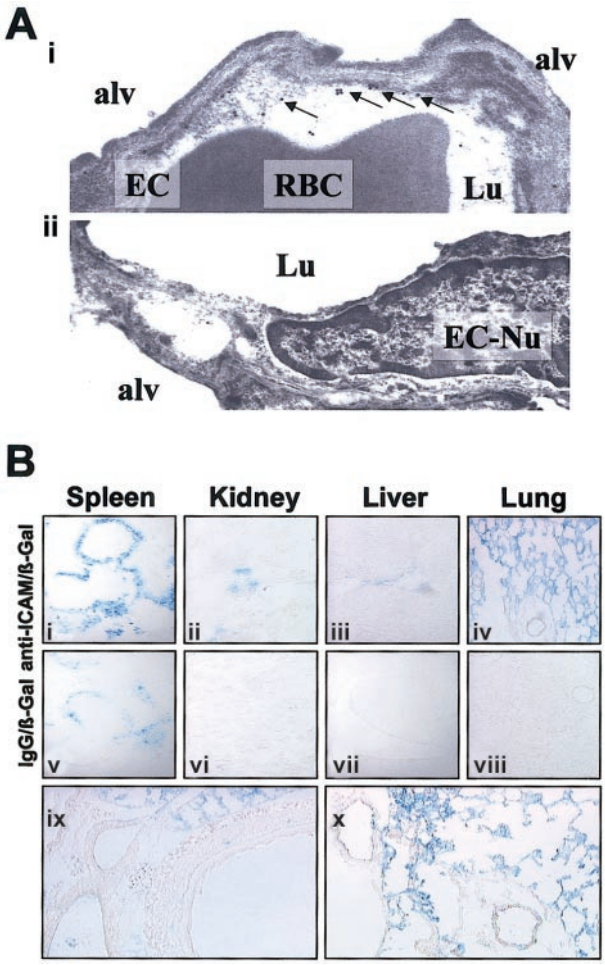


**Figure 6. Localization of anti-ICAM and anti-ICAM/β-Gal in the pulmonary vasculature after injection in mice.** (A) Immunogold electron microscopy of the lungs harvested 4 hours after intravenous injection of 100 μg anti-ICAM (i) or control IgG (ii). Arrows show endothelium-associated gold particles. RBC indicates red blood cells in a capillary lumen; Lu, vascular lumen; Alv, alveolar compartment; EC, endothelial cell; EC-Nu, endothelial cell nucleus. (B) Targeting of an active β-Gal conjugate was visualized 1 hour after injection in mice, using standard X-Gal chromogenic substrate staining protocol. Distribution of anti-ICAM/β-Gal (panels i-iv) and control IgG/β-Gal (panels v-viii). Detailed view of anti-ICAM/β-Gal in the lungs (panels ix and x). Original magnifications: Ai, × 70 000; Aii, × 60 000; Bi-Bviii, × 10; Bix-Bx, × 20.

were the renal glomeruli (Figure 6Bii), the known site of β-Gal elimination.[26,33]

However, injection of anti-ICAM/β-Gal, but not IgG/β-Gal, delivered β-Gal activity to the lungs (compare Figure 6Biv with Figure 6Bviii). Anti-ICAM/β-Gal was concentrated in the alveolar capillaries and in the lumen of larger vessels; no β-Gal activity was seen in subendothelial layers of blood vessels, interstitium, or airways (Figure 6Bix-x).

### Effect of anti-ICAM conjugate size on endothelial internalization

Streptavidin was cross-linked to biotinylated anti-ICAM and biotinylated tPA at varying molar ratios of reactants, as previously studied with other proteins.[25-27] Analysis using dynamic light scattering analysis showed that conjugates ranging in size from 100 nm to several microns were generated, depending on the molar ratio between SA and biotinylated anti-ICAM (Figure 7A). Double staining of fluorescent-labeled anti-ICAM conjugates revealed that rat microvascular endothelial cells internalized those anti-ICAM conjugates having a diameter of 100-200 nm but did not internalize large conjugates around 1 μm (Figure 7B). In fact, after a 1-hour incubation at 37°C, the large, 1-2 micron double-labeled anti-ICAM conjugates (the preparation that corresponds to the peak farthest to the right in Figure 7A) decorated the entire cell surface (Figure 7C). Control IgG conjugates did not bind to endothelium irrespective of size and did not accumulate in the isolated rat lungs (not shown).

### ICAM-directed targeting of tPA to the pulmonary vasculature

We then tested whether anti-ICAM would target an antithrombotic drug to sites of inflammation susceptible to thrombosis. To do so, we prepared large (approximately 1 μm), poorly internalizable anti-ICAM/$^{125}$I-tPA and IgG/$^{125}$I-tPA conjugates. One hour after intravenous injection, 7% of the injected anti-ICAM/$^{125}$I-tPA had accumulated in the rat lungs, compared with less than 0.3% for IgG/$^{125}$I-tPA (Figure 8A), a pulmonary $ISI_{\%ID/g}$ of 25 (Figure 8B). The blood level of anti-ICAM/$^{125}$I-tPA showed a corresponding decrease compared to IgG/$^{125}$I-tPA. Therefore, the pulmonary LR of anti-ICAM/$^{125}$I-tPA exceeded 20 (Figure 8C), with a calculated $ISI_{LR}$ of approximately 80 (Figure 8D). Anti-ICAM/$^{125}$I-tPA was retained in the lungs for at least several hours after injection (not shown). Similar results were obtained in mice (not shown).

### Anti-ICAM/tPA bound to the pulmonary endothelium surface retains plasminogen activity and dissolves intravascular clots

To test whether anti-ICAM can be used to deliver enzymatically active tPA to the endothelial lumen, we perfused anti-ICAM/tPA or

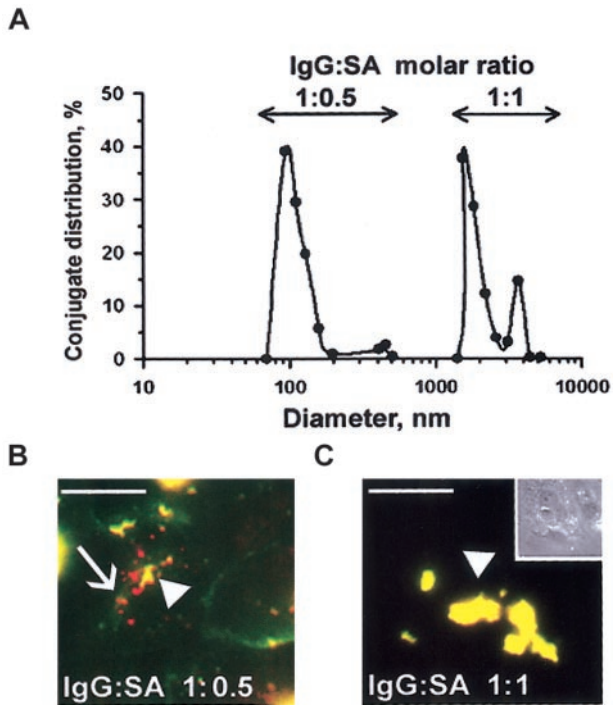


**Figure 7. Size of anti-ICAM conjugates modifies their uptake by endothelial cells.** (A) DLS analysis of size distribution of the conjugates prepared at molar ratio between biotinylated anti-ICAM and streptavidin of 1:0.5 (left peak) or 1:1 (right peak). (B-C) RPMVECs were incubated for 1 hour at 37°C with anti-ICAM conjugates containing rhodamine-labeled streptavidin with mean diameters of 100-200 nm (panel B) or larger than 1 μm (panel C). The surface-bound fraction of the conjugate was double-labeled using an FITC-labeled secondary antibody. Red color (arrows) denotes internalized conjugates; yellow color (arrowheads) denotes the noninternalizable, larger conjugates. White bars in panels B and C correspond to 5 μm size. Panel C inset shows the contrast phase micrograph (× 40) minimized to ⅓ the original size.

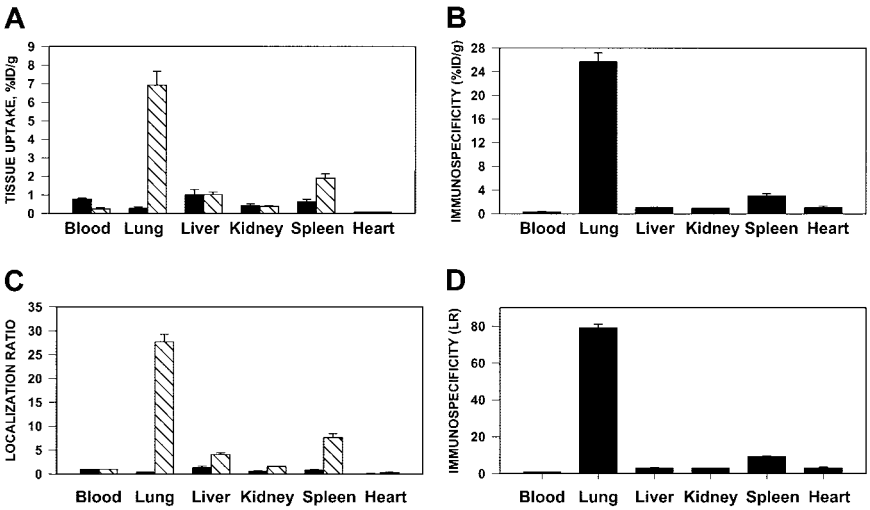


**Figure 8. Pulmonary targeting of $^{125}$I-tPA conjugated with anti-ICAM in rats.** Biodistribution of $^{125}$I-tPA conjugated to anti-ICAM IgG (▨) or control IgG (■) 1 hour after intravenous injection in anesthetized rats. The data are shown as means ± SEM, n = 4. (A) Absolute values of the uptake in organs expressed as percent of injected dose per gram. (B) Immunospecificity index ($ISI_{\%ID/g}$), calculated as ratio of anti-ICAM to IgG %ID/g. (C) Localization ratio (LR) calculated as ratio of %ID/g in an organ to that in blood. (D) $ISI_{LR}$ calculated as ratio of anti-ICAM LR to IgG LR.

IgG/tPA in IPL. In all experiments, the vasculature was washed free of unbound conjugates prior to measuring tPA uptake and activity. Anti-ICAM but not the control IgG carriage led to pulmonary accumulation of $^{125}$I-tPA (Figure 9A).

Aliquots of lung homogenates obtained after perfusion of anti-ICAM/tPA or IgG/tPA were then incubated with $^{125}$I-fibrin clots at 37°C in vitro. Homogenates of lungs perfused with anti-ICAM/tPA caused 10-fold more fibrinolysis, measured by release of $^{125}$I, than lungs perfused with IgG/tPA (Figure 9B).

We then infused a chromogenic tPA substrate into IPL. Enzymatic conversion of the substrate leading to appearance of a colored product was detected in the perfusate outflow of lungs preperfused with anti-ICAM/tPA but not those preperfused with IgG/tPA (Figure 9C). Therefore, the anti-ICAM/tPA associated with the luminal surface of the pulmonary endothelium retains its enzymatic activity.

Accessibility to a small synthetic substrate (mol wt < 500 D) does not prove that the anti-ICAM/tPA is accessible to convert its protein substrate, plasminogen. To examine this issue, a suspension of $^{125}$I-microemboli was infused into the pulmonary artery 1 hour after perfusion with either anti-ICAM/tPA or IgG/tPA. The radioactivity in the lungs was determined 1 hour later as a measure of residual unlysed fibrin clots. Lungs preperfused with anti-ICAM/tPA practically completely dissolved the radiolabeled fibrin clots, whereas fibrinolysis in the lungs perfused with IgG/tPA did not differ significantly from the basal level measured in control lungs (Figure 9D). Therefore, anti-ICAM/tPA accumulates in the lungs, resides in enzymatically active form on the luminal endothelial surface, and thereby markedly facilitates fibrinolysis in the pulmonary vasculature.

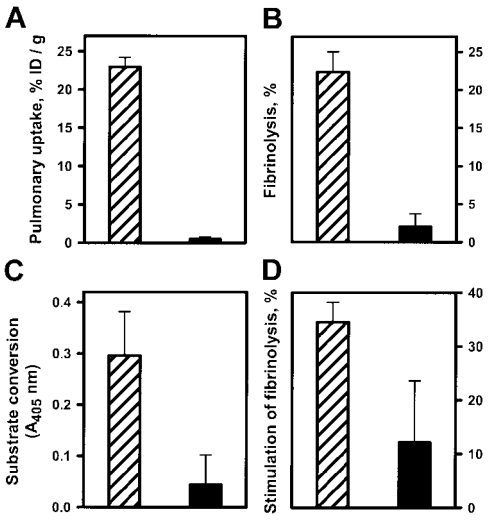


**Figure 9. Anti-ICAM/tPA accumulated in pulmonary vasculature facilitates fibrinolysis.** Isolated rat lungs were perfused with anti-ICAM/tPA (▨) or IgG/tPA (■) for 30 minutes at 37°C and washed free of unbound conjugates (5 minutes of noncirculating perfusion with a buffer). (A) Pulmonary uptake of $^{125}$I-tPA conjugated to either anti-ICAM or control IgG. (B) Fibrinolysis of fibrin clots by aliquots of lung homogenates obtained after perfusion. (C) Conversion of chromogenic tPA substrate perfused after the conjugates. (D) Dissolution of radiolabeled fibrin emboli lodged in the pulmonary vasculature after perfusion of the conjugates. The data are shown as means ± SEM, n = 4.

## Discussion

Drug targeting and concurrent blocking of a noninternalized highly expressed pro-inflammatory determinant expressed on the endothelial lumen that is stably up-regulated in the perturbed vasculature may provide a specific and powerful approach for treatment and prophylaxis of vascular inflammation and thrombosis. Our data indicate that ICAM-1 (CD54) fulfills the criteria of an "ideal" target for this specific goal and that anti-ICAM may be used for vascular immunotargeting of antithrombotic drugs.

Static human endothelial cells cultured under sterile conditions constitutively express relatively modest levels of ICAM-1 (Figure 1). However, the level of expression is much higher in vivo,[34] and anti-ICAM binds to the resting endothelium in intact animals.[20,34] Diverse cell types express ICAM-1, but the largest fraction directly accessible to the bloodstream is exposed on the endothelial surface.[34] This fact explains anti-ICAM targeting in vascularized organs (Figures 2 and 4) and confinement of the targeted cargoes to the vascular lumen (Figures 2, 6, and 9).

The pulmonary vasculature is the first major capillary network encountered by intravenously injected antibodies, contains roughly one-third of the endothelium in the body, is exposed to the entire cardiac output of venous blood, and, therefore, comprises the preferred target for affinity carriers recognizing pan-endothelial determinants.[28,31] Importantly, pulmonary uptake of anti-ICAM and anti-ICAM conjugates is not due to a nonspecific binding or mechanical retention in the vasculature, as control IgG counterparts neither bound to HUVECs nor accumulated in the lungs. In fact, the immunospecificity of the anti-ICAM and anti-ICAM/tPA conjugate pulmonary accumulation in normal rats approaches

values of 250 and 50, respectively (Figures 4 and 8). Analysis of the quantitative binding data obtained in rat lungs (Figure 2) indicates that binding of approximately 5-50 mg anti-ICAM can be expected in the human pulmonary vasculature. Thus, anti-ICAM carriers are likely to provide robust and preferential targeting to the pulmonary endothelium in intact animals, matching the characteristics of the best candidate carriers tested to date, including antibodies directed against PECAM, ACE, and a caveoli-associated antigen gp90.[15,24,28,31,33]

Certain pathological conditions suppress targeting to other constitutive endothelial determinants, such as thrombomodulin and ACE.[18,35,36] For example, endotoxin inhibits anti-ACE targeting in rats by 50% (Figure 5). In contrast, cytokines, oxidants, abnormal shear stress, and thrombin[37] are all known to enhance endothelial ICAM-1 expression[34,38] and augment anti-ICAM vascular targeting in vivo.[16,20] Up-regulation of endothelial ICAM-1 expression by thrombin[37] also makes it a preferred candidate for delivering antithrombotic agents. Our data extend these observations and reveal that (1) cytokine stimulation does not augment anti-ICAM internalization (Figure 3) and (2) pulmonary targeting of anti-ICAM is stably augmented in models of proinflammatory challenge in vivo (eg, Figure 5). This feature distinguishes targeting ICAM from targeting selectins, which are only transiently exposed on the perturbed endothelium.[39]

Antibodies and conjugates may unintentionally suppress important functions of endothelial proteins with potentially deleterious consequences (eg, thrombosis), making them less suitable for the therapeutic targeting.[40] ICAM-1, a counter-receptor for leukocyte integrins, supports cell adhesion on endothelium.[34,41] Because anti-ICAM suppresses inflammation by blocking leukocyte adhesion,[34,38,41-44] drug targeting to endothelial ICAM-1 is unlikely to have unintended deleterious effects on the host and, indeed, may provide secondary therapeutic benefits against inflammation, thrombosis, and oxidative stress. This feature of anti-ICAM conjugates deserves additional investigation.

Published studies on anti-ICAM internalization have yielded inconsistent results: epithelial and blood cells have been reported to internalize ICAM ligands in vitro,[45,46] but fragmentary data in other cell types showed the opposite outcome.[47,48] Our studies in cell culture, perfused rat lungs, and in animals show that endothelial cells internalize ICAM antibodies poorly (Figures 1, 2, 3, and 6). Thus, ICAM seems to be well suited for drug targeting to the luminal surface. This feature distinguishes ICAM from other similarly prevalent endothelial determinants, all of which are rapidly internalized, including thrombomodulin and ACE (Figures 1 and 2), selectins,[47-50] and caveoli-associated antigens.[15] A monoclonal antibody against gp85 antigen accumulates in the rat lungs and is not internalized and therefore can be used for surface targeting in this species,[29] but the identity, function, and regulation of its human counterpart are not known.

The uptake of anti-ICAM conjugates is modified by their size: endothelium internalizes conjugates with a mean diameter of 100-200 nm, but not anti-ICAM conjugates larger than 1 μm (Figure 7). This result indicates that anti-ICAM follows the paradigm observed previously with antibodies directed against another noninternalizable determinant, PECAM-1.[26-28] Conjugate size can be readily and stably modulated by varying the molar ratios of the reactants, as measured by dynamic light scattering (Figure 7). In theory, therefore, anti-ICAM represents a carrier that can be modified to facilitate drug delivery to either the endothelial surface (using monomolecular conjugates or conjugates larger than 500 nm) or to the intracellular compartment (using 100-300 nm conjugates). The anti-ICAM/tPA conjugates used in the present study were around 1 μm in size, which exceeds the effective internalizable size. Clearly, anti-ICAM/tPA bound along the cell surface retains enzymatic activity in the pulmonary vascular lumen and augments intravascular fibrinolysis (Figure 9).

This result serves as a proof-of-principle that ICAM represents a suitable target to deliver antithrombotic agents to the endothelial lumen. Although anti-ICAM/tPA conjugate itself may represent a useful agent, we anticipate that the strategy can be further optimized by generation of a monomolecular noninternalizable anti-ICAM/tPA fusion protein.

To our knowledge this is the first study showing that fibrinolytic agents can be used in a prophylactic mode to protect vital vascular beds, including those in the lungs. Patients are at high risk to develop pulmonary emboli after trauma: (1) when extensive proximal deep venous thrombi are present; (2) after recent pulmonary emboli; (3) in the setting serious respiratory compromise due to diverse cardiopulmonary disease; or (4) when the risk of bleeding after systemic anticoagulation is prohibitive.[1,2] Our data suggest that targeted delivery of antithrombotic agents to the pulmonary endothelium itself may be a suitable alternative in some of these settings, although additional studies will be needed to establish the duration and extent of fibrinolytic activity that is delivered.

In summary, ICAM possesses a number of highly desirable characteristics as a target for antithrombotic and anti-inflammatory drug delivery. Anti-ICAM targeting may allow a spectrum of novel therapeutic approaches, for example, a strategy to facilitate the antithrombotic potential of the pulmonary vasculature in patients at high risk to develop acute lung injury (ALI/ARDS) and thromboembolism. Future studies in larger animals will define potential therapeutic applicability and limitations of this strategy.

## Acknowledgments

The authors appreciate the gift of anti-ACE from Dr S. Danilov (University of Illinois in Chicago) and anti-TM from Drs C. Esmon (Oklahoma Medial Research Foundation) and S. Kennel (National Oakridge Laboratory).

## References

1. Bergqvist D, Agnelli G, Cohen AT, et al. Duration of prophylaxis against venous thromboembolism with enoxaparin after surgery for cancer. N Engl J Med. 2002;346:975-980.
2. Decousus H, Leizorovicz A, Parent F, et al. A clinical trial of vena caval filters in the prevention of pulmonary embolism in patients with proximal deep-vein thrombosis: Prevention du Risque d'Embolie Pulmonaire par Interruption Cave Study Group. N Engl J Med. 1998;338:409-415.
3. Lang IM, Marsh JJ, Olman MA, Moser KM, Loskutoff DJ, Schleef RR. Expression of type 1 plasminogen activator inhibitor in chronic pulmonary thromboemboli. Circulation. 1994;89:2715-2721.
4. Holvoet P, Dewerchin M, Stassen JM, et al. Thrombolytic profiles of clot-targeted plasminogen activators: parameters determining potency and initial and maximal rates. Circulation. 1993; 87:1007-1016.
5. Runge MS, Harker LA, Bode C, et al. Enhanced thrombolytic and antithrombotic potency of a fibrin-targeted plasminogen activator in baboons. Circulation. 1996;94:1412-1422.
6. Sakharov DV, Rijken DC. Superficial accumulation of plasminogen during plasma clot lysis. Circulation. 1995;92:1883-1890.
7. Muller DW, Gordon D, San H, et al. Catheter-mediated pulmonary vascular gene transfer and expression. Circ Res. 1994;75:1039-1049.
8. Dichek DA, Anderson J, Kelly AB, Hanson SR, Harker LA. Enhanced in vivo antithrombotic effects of endothelial cells expressing recombinant

plasminogen activators transduced with retroviral vectors. Circulation. 1996;93:301-309.

9. Waugh JM, Kattash M, Li J, et al. Gene therapy to promote thromboresistance: local overexpression of tissue plasminogen activator to prevent arterial thrombosis in an in vivo rabbit model. Proc Natl Acad Sci U S A. 1999;96:1065-1070.
10. Carmeliet P, Stassen JM, Van Vlaenderen I, Meidell RS, Collen D, Gerard RD. Adenovirus-mediated transfer of tissue-type plasminogen activator augments thrombolysis in tissue-type plasminogen activator-deficient and plasminogen activator inhibitor-1-overexpressing mice. Blood. 1997;90: 1527-1534.
11. Kennel SJ, Lee R, Bultman S, Kabalka G. Rat monoclonal antibody distribution in mice: an epitope inside the lung vascular space mediates very efficient localization. Int J Rad Appl Instrum B. 1990;17:193-200.
12. Keelan ET, Harrison AA, Chapman PT, Binns RM, Peters AM, Haskard DO. Imaging vascular endothelial activation: an approach using radiolabeled monoclonal antibodies against the endothelial cell adhesion molecule E-selectin. J Nucl Med. 1994;35:276-281.
13. Harari OA, Wickham TJ, Stocker CJ, et al. Targeting an adenoviral gene vector to cytokine-activated vascular endothelium via E-selectin. Gene Ther. 1999;6:801-807.
14. Lindner JR, Song J, Christiansen J, Klibanov AL, Xu F, Ley K. Ultrasound assessment of inflammation and renal tissue injury with microbubbles targeted to P-selectin. Circulation. 2001;104:2107-2112.
15. McIntosh DP, Tan XY, Oh P, Schnitzer JE. Targeting endothelium and its dynamic caveolae for tissue-specific transcytosis in vivo: a pathway to overcome cell barriers to drug and gene delivery. Proc Natl Acad Sci U S A. 2002;99:1996-2001.
16. Panes J, Perry MA, Anderson DC, et al. Regional differences in constitutive and induced ICAM-1 expression in vivo. Am J Physiol. 1995;269: H1955-H1964.
17. Bloemen PG, Henricks PA, van Bloois L, et al. Adhesion molecules: a new target for immunoliposome-mediated drug delivery. FEBS Lett. 1995;357:140-144.
18. Atochina EN, Balyasnikova IV, Danilov SM, Granger DN, Fisher AB, Muzykantov VR. Immunotargeting of catalase to ACE or ICAM-1 protects perfused rat lungs against oxidative stress. Am J Physiol. 1998;275:L806-L817.
19. Weiner RE, Sasso DE, Gionfriddo MA, et al. Early detection of bleomycin-induced lung injury in rat using indium-111-labeled antibody directed against intercellular adhesion molecule-1 [published erratum appears in J Nucl Med. 1998;39: 869]. J Nucl Med. 1998;39:723-728.
20. Villanueva FS, Jankowski RJ, Klibanov S, et al. Microbubbles targeted to intercellular adhesion molecule-1 bind to activated coronary artery endothelial cells. Circulation. 1998;98:1-5.
21. Marlin SD, Springer TA. Purified intercellular adhesion molecule-1 (ICAM-1) is a ligand for lymphocyte function-associated antigen 1 (LFA-1). Cell. 1987;51:813-819.
22. Christensen PJ, Kim S, Simon RH, Toews GB, Paine R. Differentiation-related expression of ICAM-1 by rat alveolar epithelial cells. Am J Resp Cell Mol Biol. 1993;8:9-15.
23. Jevnikar AM, Wuthrich RP, Takei F, et al. Differing regulation and function of ICAM-1 and class II antigens on renal tubular cells. Kidney Int. 1990; 38:417-425.
24. Danilov SM, Muzykantov VR, Martynov AV, et al. Lung is the target organ for a monoclonal antibody to angiotensin-converting enzyme. Lab Invest. 1991;64:118-124.
25. Muzykantov VR, Barnathan ES, Atochina EN, Kuo A, Danilov SM, Fisher AB. Targeting of antibody-conjugated plasminogen activators to the pulmonary vasculature. J Pharmacol Exp Ther. 1996;279:1026-1034.
26. Scherpereel A, Wiewrodt R, Christofidou-Solomidou M, et al. Cell-selective intracellular delivery of a foreign enzyme to endothelium in vivo using vascular immunotargeting. FASEB J. 2001;15: 416-426.
27. Wiewrodt R, Thomas AP, Cipelletti L, et al. Size-dependent intracellular immunotargeting of therapeutic cargoes into endothelial cells. Blood. 2002; 99:912-922.
28. Muzykantov VR, Christofidou-Solomidou M, Balyasnikova I, et al. Streptavidin facilitates internalization and pulmonary targeting of an anti-endothelial cell antibody (platelet-endothelial cell adhesion molecule 1): a strategy for vascular immunotargeting of drugs. Proc Natl Acad Sci U S A. 1999;96:2379-2384.
29. Murciano JC, Harshaw DW, Ghitescu L, Danilov SM, Muzykantov VR. Vascular immunotargeting to endothelial surface in a specific macrodomain in alveolar capillaries. Am J Resp Crit Care Med. 2001;164:1295-1302.
30. Murciano JC, Harshaw D, Neschis DG, et al. Platelets inhibit the lysis of pulmonary microemboli. Am J Physiol Lung Cell Mol Physiol. 2002; 282:L529-L539.
31. Danilov SM, Gavrilyuk VD, Franke FE, et al. Lung uptake of antibodies to endothelial antigens: key determinants of vascular immunotargeting. Am J Physiol Lung Cell Mol Physiol. 2001;280:L1335-L1347.
32. Bdeir K, Murciano JC, Tomaszewski J, et al. Urokinase mediates fibrinolysis in the pulmonary microvasculature. Blood. 2000;96:1820-1826.
33. Scherpereel A, Rome JJ, Wiewrodt R, et al. Platelet-endothelial cell adhesion molecule-1-directed immunotargeting to cardiopulmonary vasculature. J Pharmacol Exp Ther. 2002;300: 777-786.
34. Dustin ML, Rothlein R, Bhan AK, Dinarello CA, Springer TA. Induction by IL 1 and interferon-gamma: tissue distribution, biochemistry, and function of a natural adherence molecule (ICAM-1). J Immunol. 1986;137:245-254.
35. Atochina EN, Hiemisch HH, Muzykantov VR, Danilov SM. Systemic administration of platelet-activating factor in rat reduces specific pulmonary uptake of circulating monoclonal antibody to angiotensin-converting enzyme. Lung. 1992;170: 349-358.
36. Moore KL, Esmon CT, Esmon NL. Tumor necrosis factor leads to the internalization and degradation of thrombomodulin from the surface of bovine aortic endothelial cells in culture. Blood. 1989;73:159-165.
37. Kaplanski G, Marin V, Fabrigoule M, et al. Thrombin-activated human endothelial cells support monocyte adhesion in vitro following expression of intercellular adhesion molecule-1 (ICAM-1; CD54) and vascular cell adhesion molecule-1 (VCAM-1; CD106). Blood. 1998;92:1259-1267.
38. Kumasaka T, Quinlan WM, Doyle NA, et al. Role of the intercellular adhesion molecule-1(ICAM-1) in endotoxin-induced pneumonia evaluated using ICAM-1 antisense oligonucleotides, anti-ICAM-1 monoclonal antibodies, and ICAM-1 mutant mice. J Clin Invest. 1996;97:2362-2369.
39. Fries JW, Williams AJ, Atkins RC, Newman W, Lipscomb MF, Collins T. Expression of VCAM-1 and E-selectin in an in vivo model of endothelial activation. Am J Pathol. 1993;143:725-737.
40. Christofidou-Solomidou M, Kennel S, Scherpereel A, et al. Vascular immunotargeting of glucose oxidase to the endothelial antigens induces distinct forms of oxidant acute lung injury: targeting to thrombomodulin, but not to PECAM-1, causes pulmonary thrombosis and neutrophil transmigration. Am J Pathol. 2002;160:1155-1169.
41. Diamond MS, Staunton DE, de Fougerolles AR, et al. ICAM-1 (CD54): a counter-receptor for Mac-1 (CD11b/CD18). J Cell Biol. 1990;111: 3129-3139.
42. DeMeester SR, Molinari MA, Shiraishi T, et al. Attenuation of rat lung isograft reperfusion injury with a combination of anti-ICAM-1 and anti-beta2 integrin monoclonal antibodies. Transplantation. 1996;62:1477-1485.
43. Broide DH, Humber D, Sullivan S, Sriramarao P. Inhibition of eosinophil rolling and recruitment in P-selectin- and intracellular adhesion molecule-1-deficient mice. Blood. 1998;91:2847-2856.
44. Broide DH, Sullivan S, Gifford T, Sriramarao P. Inhibition of pulmonary eosinophilia in P-selectin- and ICAM-1-deficient mice. Am J Respir Cell Mol Biol. 1998;18:218-225.
45. Mastrobattista E, Storm G, van Bloois L, et al. Cellular uptake of liposomes targeted to intercellular adhesion molecule-1 (ICAM-1) on bronchial epithelial cells. Biochim Biophys Acta. 1999;1419: 353-363.
46. Gursoy RN, Siahaan TJ. Binding and internalization of an ICAM-1 peptide by the surface receptors of T cells. J Pept Res. 1999;53:414-421.
47. Almenar-Queralt A, Duperray A, Miles LA, Felez J, Altieri DC. Apical topography and modulation of ICAM-1 expression on activated endothelium. Am J Pathol. 1995;147:1278-1288.
48. von Asmuth EJ, Smeets EF, Ginsel LA, Onderwater JJ, Leeuwenberg JF, Buurman WA. Evidence for endocytosis of E-selectin in human endothelial cells. Eur J Immunol. 1992;22:2519-2526.
49. Kuijpers TW, Raleigh M, Kavanagh T, et al. Cytokine-activated endothelial cells internalize E-selectin into a lysosomal compartment of vesiculotubular shape: a tubulin-driven process. J Immunol. 1994;152:5060-5069.
50. Spragg DD, Alford DR, Greferath R, et al. Immunotargeting of liposomes to activated vascular endothelial cells: a strategy for site-selective delivery in the cardiovascular system. Proc Natl Acad Sci U S A. 1997;94:8795-8800.